Very-high-energy emission of the Crab Pulsar and tests for Lorentz Invariance Violation

Anna Campoy-Ordaz[1,2], Markus Gaug[1,2],
on behalf of the MAGIC Collaboration

[1] Institut d’Estudis Espacials de Catalunya (IEEC), Spain

[2] Universitat Autònoma de Barcelona (UAB), Spain

03.09.2026 | TeV Particle Astrophysics 2026

Contents

I. Lorentz Invariance Violation

- Modified photon dispersion relation

$$E^2 = p^2c^2 \times \left[1 + \sum_{n=1}^{\infty} S_n \left(\frac{E}{E_{QG,n}}\right)^n\right]$$

$S_n = +1$, superluminal
$S_n = -1$, subluminal

$n = 1$, linear case
$n = 2$, quadratic case

- Energy-dependent photon group velocity

$$v_\gamma = \frac{\partial E}{\partial p} \simeq c \left[1 + \sum_{n=1}^{\infty} S_n \frac{n+1}{2} \left(\frac{E}{E_{QG,n}}\right)^n\right]$$

I. Lorentz Invariance Violation

- Energy-dependent time delay

$$\Delta t_n \simeq S_n \frac{n+1}{2} \frac{E_h^n - E_l^n}{H_0 E_{QG}^n} \kappa_n(z)$$

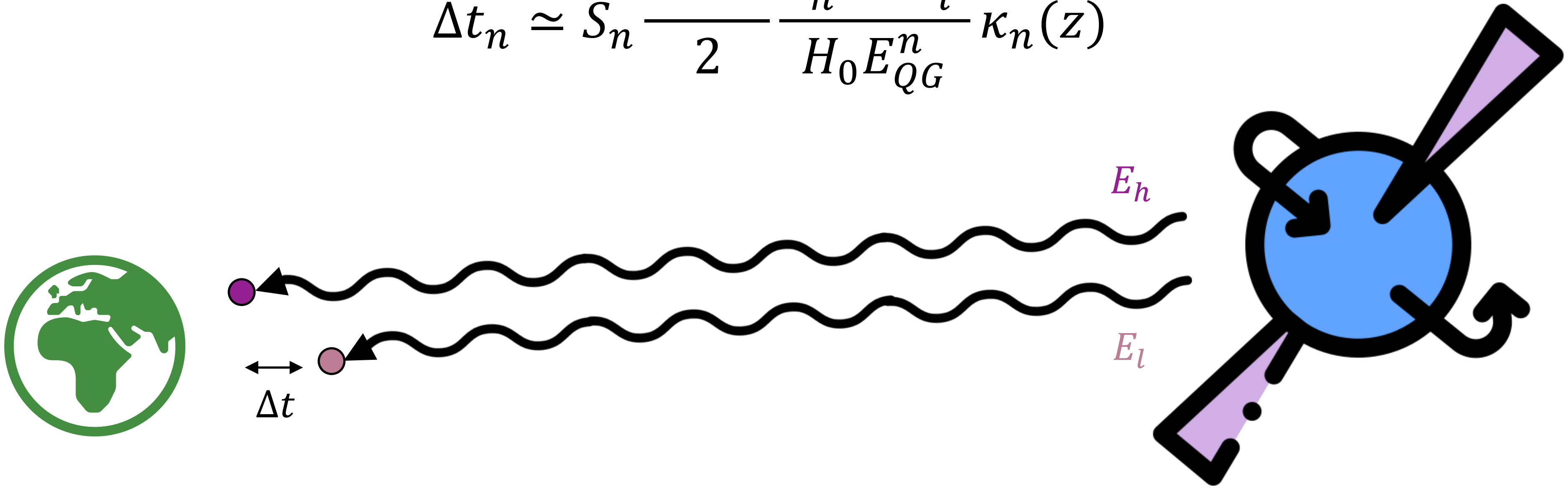

I. Lorentz Invariance Violation

- Energy-dependent phase delay

$$\Delta\phi = \frac{d_{Crab}}{cP_{Crab}} \cdot S_n \frac{n+1}{2} \frac{E_h^n - E_l^n}{E_{QG}^n}$$

- Bounds to $E_{QG,n}$

$$E_{QG,n} \gtrsim \left(S_n \frac{n+1}{2} \frac{d_{Crab}}{cP_{Crab}} \frac{E_h^n - E_l^n}{\Delta\phi} \right)^{1/n}$$

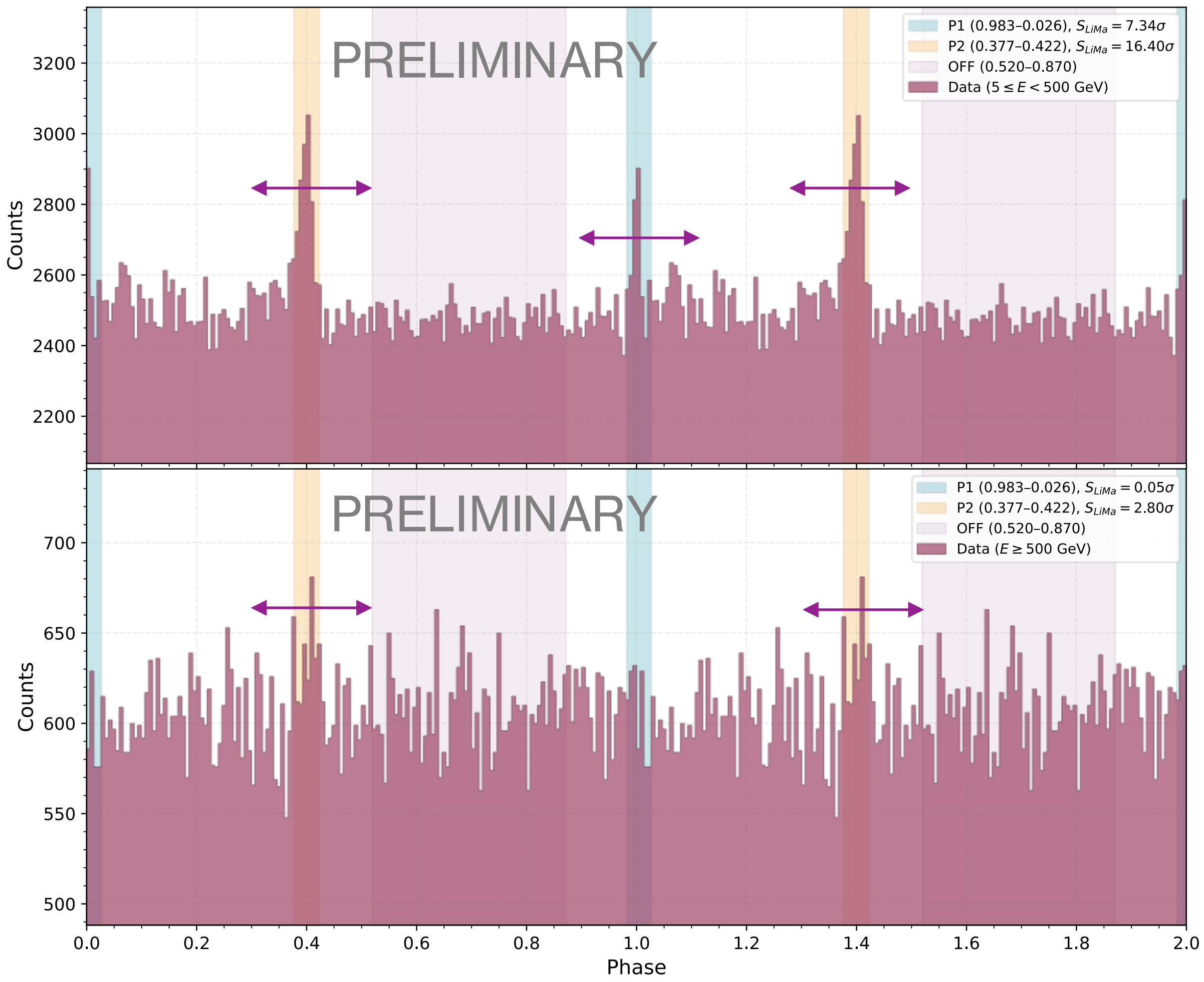

i. Competitivity of LIV searches

- Active Galactic Nuclei (AGNs)
- Gamma-Ray Bursts (GRBs)

At cosmological distances, BUT maximum observable energy is limited by the Extragalactic Background Light

- Pulsars

Independent of the cosmological model

Source family	Distance [kpc]	Energy [GeV]	δt [s]	Expected bounds	
				$E_{QG,1}$	$E_{QG,2}$
AGN	$10^5 - 10^6$	10^4	$10^2 - 10^5$	$10^{15} - 10^{18}$	$10^9 - 10^{11}$
GRB	$10^5 - 10^7$	10^3	$10^0 - 10^2$	$10^{17} - 10^{19}$	$10^9 - 10^{10}$
Pulsar	$10^0 - 10^1$	10^2	$10^{-4} - 10^{-2}$	$10^{17} - 10^{19}$	$10^{10} - 10^{11}$

i. Competitivity of LIV searches

- Active galactic nuclei (AGNs)
- Gamma-ray bursts (GRBs)
- Pulsars →
  - Precisely timed flux oscillations
  - Stable source
  - ➢ **Sensitivity to LIV can be systematically planned**

Source family	Distance [kpc]	Energy [GeV]	δt [s]	Expected bounds	
				$E_{QG,1}$	$E_{QG,2}$
AGN	$10^5 - 10^6$	10^4	$10^2 - 10^5$	$10^{15} - 10^{18}$	$10^9 - 10^{11}$
GRB	$10^5 - 10^7$	10^3	$10^0 - 10^2$	$10^{17} - 10^{19}$	$10^9 - 10^{10}$
Pulsar	$10^0 - 10^1$	10^2	$10^{-4} - 10^{-2}$	$10^{17} - 10^{19}$	$10^{10} - 10^{11}$

ii. Bounds on LIV from the Crab Pulsar

Guerrero, Campoy-Ordaz, Potting, Gaug (2025)

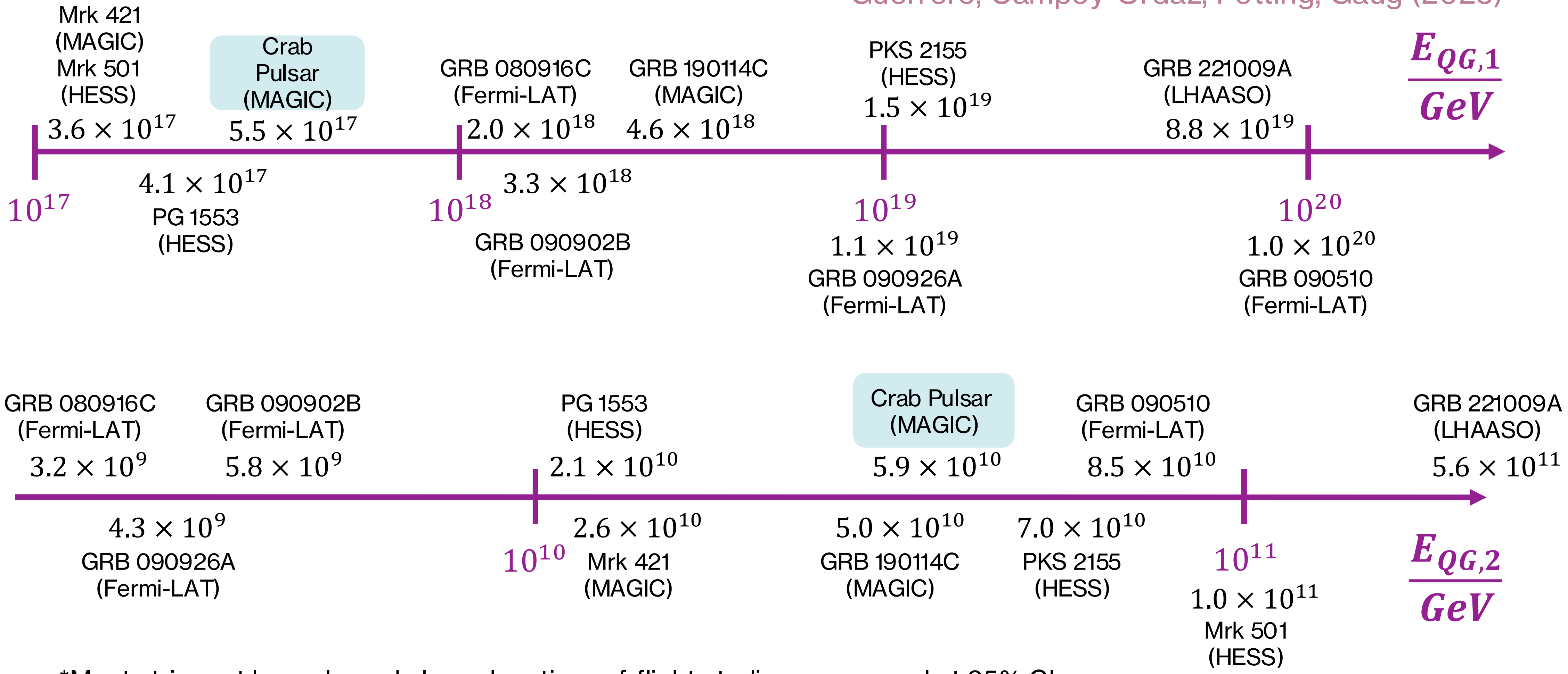

*Most stringent lower bounds based on time-of-flight studies, expressed at 95% CL.

II. Crab Pulsar Analysis

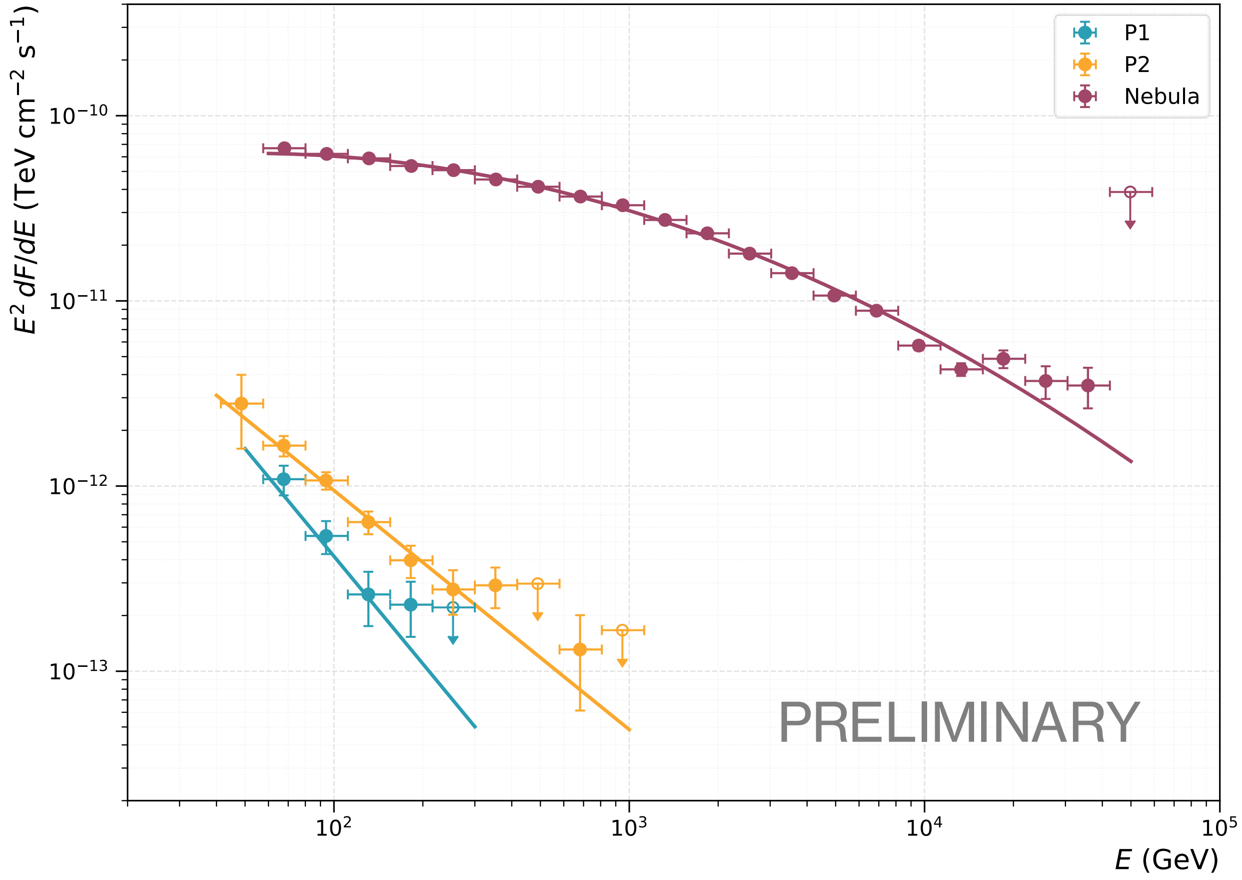

- MAGIC Telescopes
- 2009 to 2020
- ~300 hours of effective time
- Joining 11 different observation periods
- Only P2 for LIV studies
- Profile Maximum Likelihood Method

II. Crab Pulsar Analysis

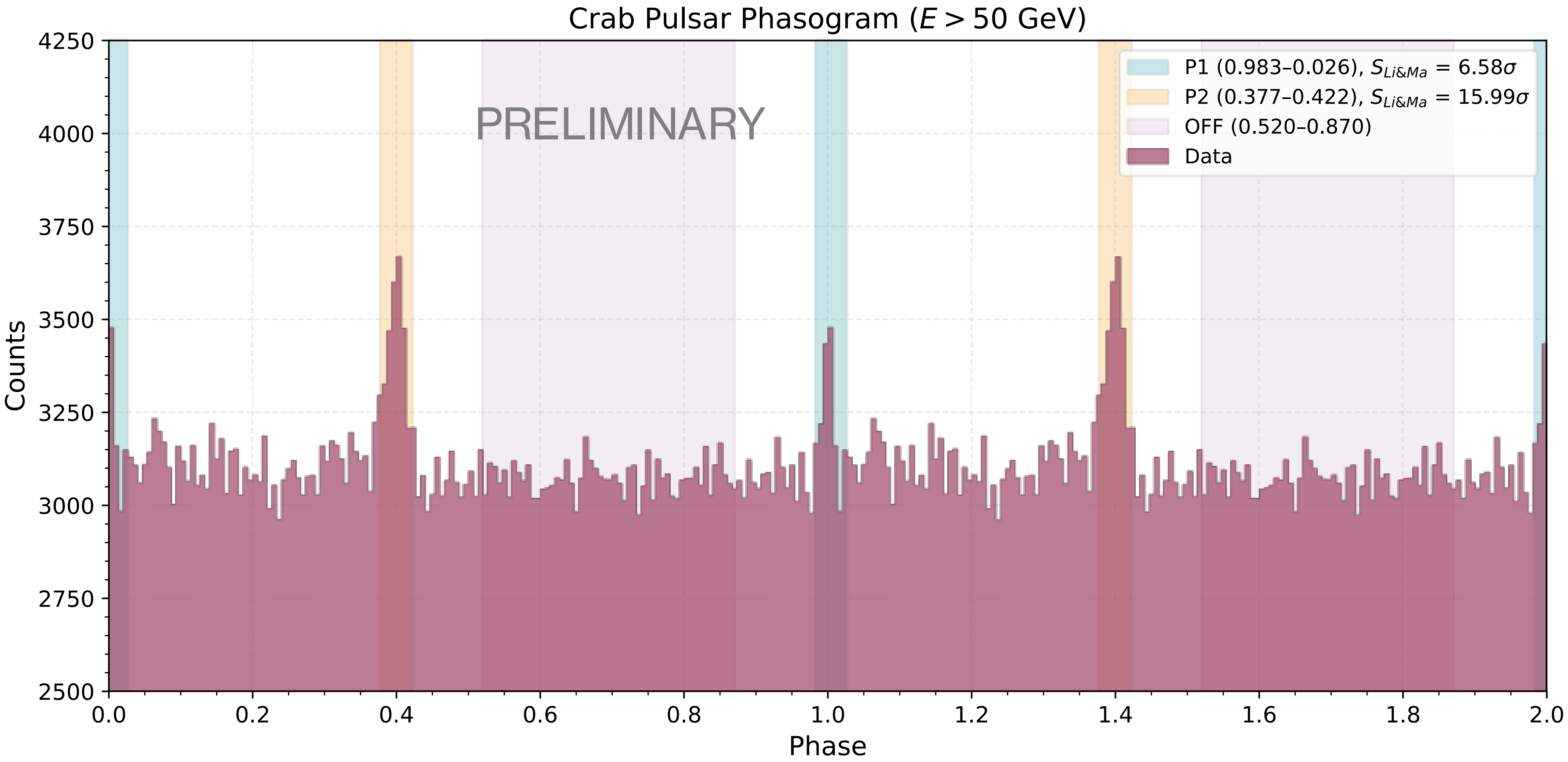

II. Crab Pulsar LIV Analysis

$$\mathcal{L}(\lambda_n; \nu | X) = \mathcal{L}(\lambda_n; f, \alpha, \phi_{P2}, \sigma_{P2} | \{E_i', \phi_i', k_i\})$$

LIV effect intensity

$\lambda_1 \equiv {10^{19}\mathrm{GeV}}/{E_{QG_1}}$

$\lambda_2 \equiv {10^{12}\mathrm{GeV}}/{E_{QG_2}}$

Nuisance parameters

f : P2 flux normalization
α : P2 spectral index
ϕ_{P2} : Mean P2 pulse position
σ_{P2} : Mean P2 width

Signal PDF → Pulsar phaseogram model for a given λ_n

- **Symmetric Gaussian**
- **Symmetric Lorentzian**
- **Asymmetric Gaussian**
- **Asymmetric Lorentzian**

a : Asymmetry parameter

II. Crab Pulsar LIV Analysis

Asymmetric Gaussian

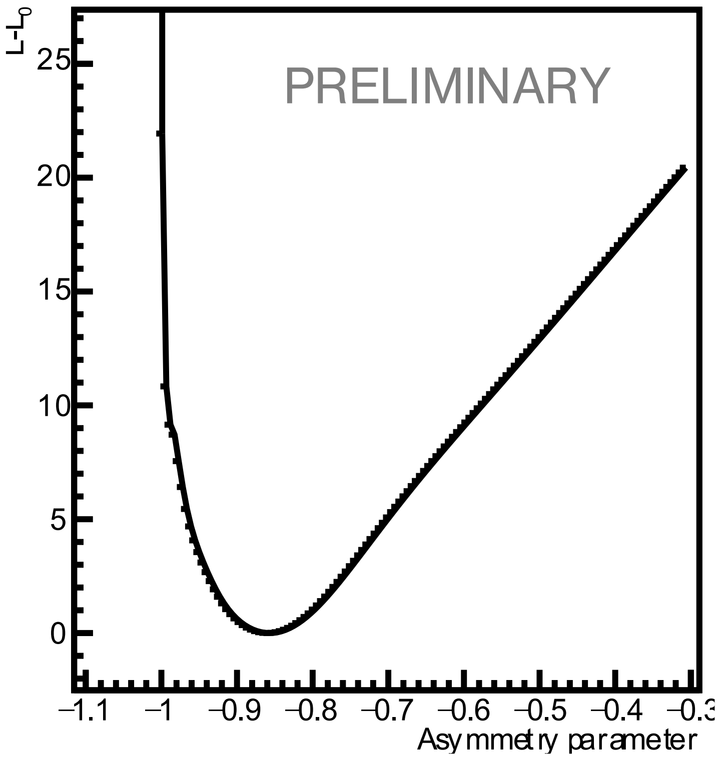

Asymmetric Lorentzian

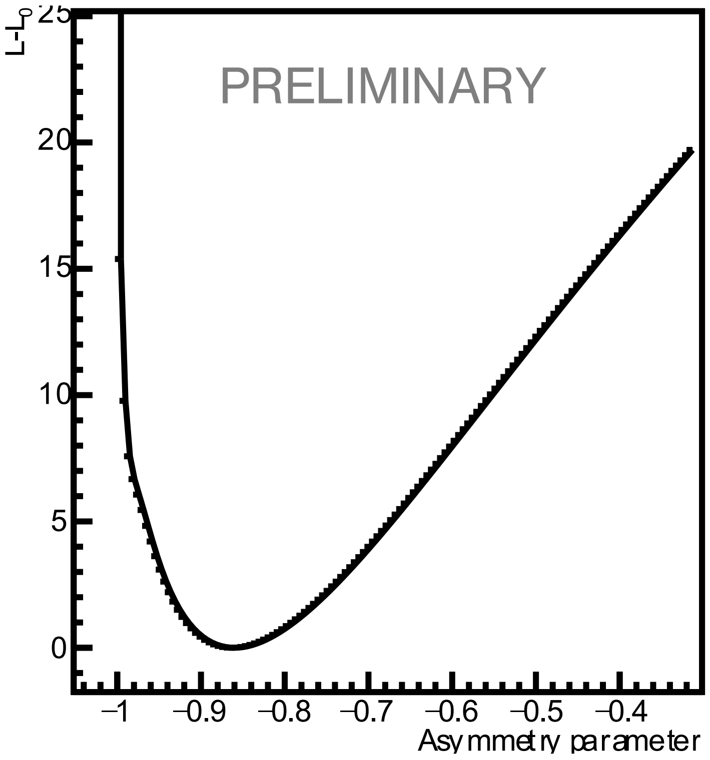

- Asymmetric Gaussian pulse shape provides a significantly better fit than the symmetric Gaussian model ($\mathbf{3.2\sigma}$)
- Asymmetric Lorentzian pulse shape is significantly preferred over the symmetric Lorentzian model ($\mathbf{3.3\sigma}$)
- Asymmetric Lorentzian moderately preferred over asymmetric Gaussian ($\boldsymbol{\Delta AIC = 3.1}$)

II. Crab Pulsar LIV Analysis

PRELIMINARY

This work

Case	$E_{QG,1}$ (GeV)
$S_1 = +1$	3.5×10^{17}
$S_1 = -1$	1.5×10^{18}
	$E_{QG,2}$ (GeV)
$S_2 = +1$	1.8×10^{10}
$S_2 = -1$	6.1×10^{10}

95% CL bounds from the Profile Likelihood Method (*without systematics)

*Asymmetric Lorentzian pulse shape with the asymmetry parameter fixed.

II. Crab Pulsar LIV Analysis

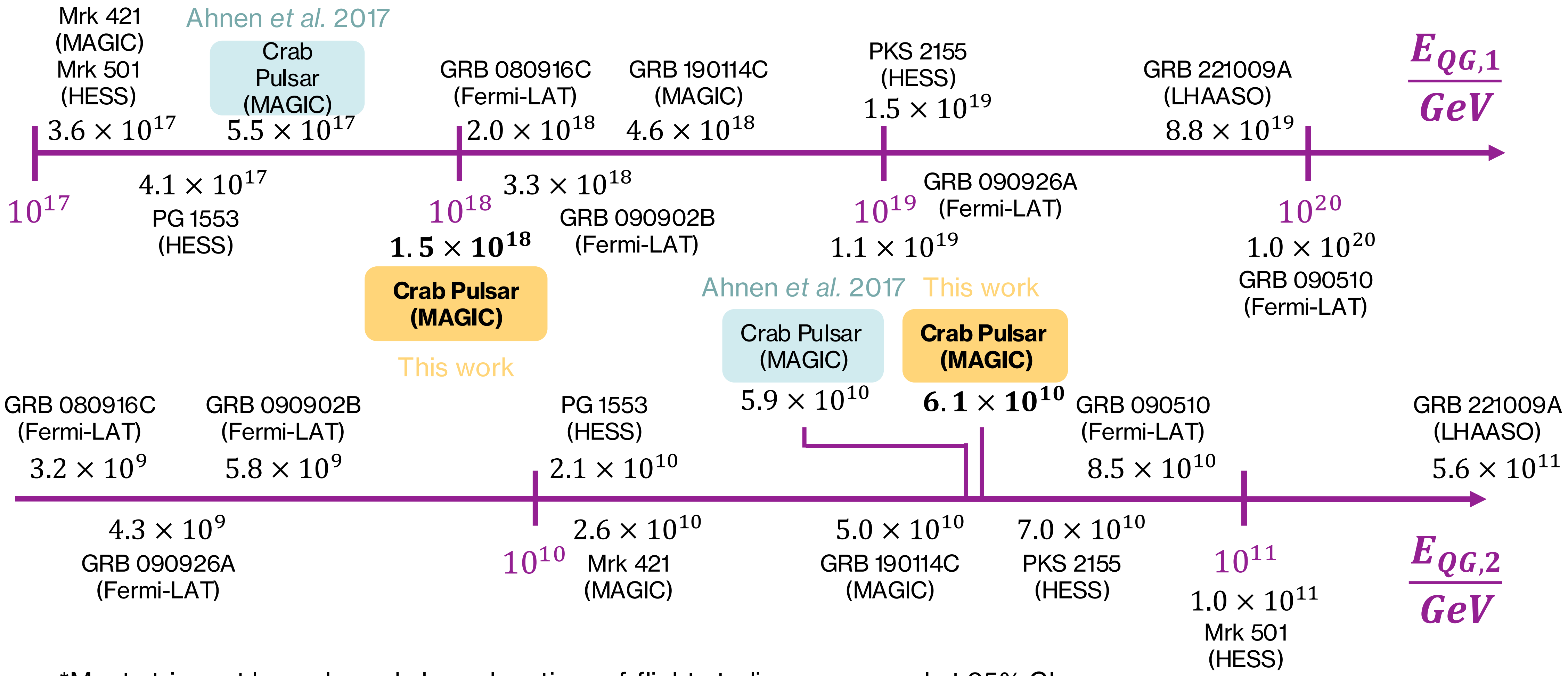

*Most stringent lower bounds based on time-of-flight studies, expressed at 95% CL.

III. Conclusions

- Spectral analysis:
  - Results marginally compatible with Ansoldi *et al.* 2016

- LIV analysis:
  - <u>Asymmetry of the pulse shape</u>
  - Results compatible with Ahnen *et al.* 2017

- General outlook:
  - Plan observations to improve the sensitivity
  - Upcoming CTAO
  - Joint LIV analysis: LIVelihood

Thank you for your attention!

i. Amelino-Camelia, G., & Smolin, L. (2009). **Prospects for constraining quantum gravity dispersion with near term observations.** *Phys. Rev. D*, *80*(8), 084017.

ii. Otte, A. (2012). **Prospects of performing Lorentz invariance tests with VHE emission from pulsars.** *Proceedings of the 32nd International Cosmic Ray Conference (ICRC 2011), 7*.

iii. Guerrero, M., Campoy-Ordaz, A., Potting, R., Gaug, M. (2025). **Bounding anisotropic Lorentz invariance violation from measurements of the effective energy scale of quantum gravity.** *Phys. Rev. D, 112*(10), 104002.

iv. Ansoldi *et al.* 2016. **Teraelectronvolt pulsed emission from the Crab Pulsar detected by MAGIC.** *Astronomy & Astrophysics*, *585*, A133.

v. Ahnen *et al.* 2017. **Constraining Lorentz Invariance Violation Using the Crab Pulsar Emission Observed up to TeV Energies by MAGIC.** *ApJS,* 232, 9.

BACK UP

II. Crab Pulsar LIV Analysis

Ahnen *et al.* 2017

Fitting both ON and OFF regions

$$\mathcal{L}(\lambda_n;\boldsymbol{\nu}|\boldsymbol{X}) = \mathcal{L}(\lambda_n; f, \alpha, \phi_{P2}, \sigma_{P2}|\{\{E'_i,\phi'_i\}_{i=0}^{N_k}\}_{k=0}^{N_s})$$

$$= P(\boldsymbol{\nu}) \cdot \prod_{k=0}^{N_s} \exp\left(-g_k(\lambda_n;\boldsymbol{\nu}) - b_k \cdot \frac{1+\tau}{\tau}\right) \cdot \prod_{m=0}^{N_k^{OFF}} b_k \cdot \prod_{i=0}^{N_k^{ON}} \left(g_k(\lambda_n;\boldsymbol{\nu}) + b_k/\tau\right) \cdot \mathcal{P}_k(E'_i,\phi'_i|\lambda_n;\boldsymbol{\nu}) \ ,$$

Individual event PDF depends on:
(fitted) background spectral energy distribution h(E') and PDF of the signal S(E', Φ'|λ_n;ν)

$$\mathcal{P}_k(E'_i,\phi'_i|\lambda_n;\boldsymbol{\nu}) = \frac{b_k/\tau \cdot h_k(E') \ + \ g_k(\lambda_n;\boldsymbol{\nu}) \cdot S_k(E'_i,\phi'_i|\lambda_n;\boldsymbol{\nu})}{g_k(\lambda_n;\boldsymbol{\nu}) \ + \ b_k/\tau}$$

Uses signal normalization $\mathbf{g_k}$ (which depends on all nuisance parameters!) and background norm $\mathbf{b_k/\tau}$

II. Crab Pulsar LIV Analysis

Ahnen *et al.* 2017

$$\mathcal{L}(\lambda_n;\boldsymbol{\nu}|\boldsymbol{X}) = \mathcal{L}(\lambda_n; f, \alpha, \phi_{P2}, \sigma_{P2}|\{\{E'_i, \phi'_i\}_{i=0}^{N_k}\}_{k=0}^{N_s})$$

$$= P(\boldsymbol{\nu}) \cdot \prod_{k=0}^{N_s} \exp\left(-g_k(\lambda_n;\boldsymbol{\nu}) - b_k \cdot \frac{1+\tau}{\tau}\right) \cdot \prod_{m=0}^{N_k^{OFF}} b_k \cdot \prod_{i=0}^{N_k^{ON}} (g_k(\lambda_n;\boldsymbol{\nu}) + b_k/\tau) \cdot \mathcal{P}_k(E'_i, \phi'_i|\lambda_n;\boldsymbol{\nu}) \ ,$$

PDF of the signal:

$$S_k\left(E'_i, \phi'_i \mid \lambda_n; \nu\right) = \frac{\Delta t_k \int_0^\infty R_k(E \mid E'_i) \cdot \Gamma_{P2}(E, f, \alpha) \cdot F_{P2}(\phi'_i, E \mid \lambda_n; \phi_{P2}, \sigma_{P2}) dE}{g_k(\lambda_n; \nu)},$$

With Γ_{P2}: pulsar spectrum & F_{P2}: **pulsar phaseogram model**.

II. Crab Pulsar LIV Analysis

- Asymmetric Lorentzian

$$f(x) = \begin{cases} \dfrac{A}{\pi}\dfrac{\sigma_1}{(x-x_0)^2+\sigma_1^2}+C, & x < x_0 \\ \dfrac{A}{\pi}\dfrac{\sigma_2}{(x-x_0)^2+\sigma_2^2}\dfrac{\sigma_2}{\sigma_1}\left(1+\dfrac{\pi\sigma_1 C}{A}\right), & x > x_0 \end{cases}$$

$$\boxed{\sigma_2 = \sigma_1 \cdot (1+a)}$$

Asymmetry parameter